이학석사 학위논문

Synthesis of Pd–Pt–Fe_3O_4 nanoflakes and their performance as magnetically recyclable catalysts for nitroarene reduction

재활용 가능한 초상자성 팔라듐-백금-산화철 나노촉매입자의 합성 및 효과적인 니트로 환원반응 적용

2016년 8월

서울대학교 대학원
화학부 유기화학 전공
송 예 미

CONTENTS

Abstract

Synthesis of Pd–Pt–Fe_3O_4 nanoflakes and their performance as magnetically recyclable catalysts for nitroarene reduction

Yea-Mi Song
Department of Chemistry and Organic Chemistry
The Graduate School
Seoul National University

Magnetically recyclable nanoparticles have attracted increasing interest for the development of efficient heterogeneous catalysts designed for practical organic synthesis. Herein, we describe the study on the synthesis of bimetallic Pd–Pt–Fe_3O_4 nanoflake-shaped nanoparticles and their catalytic applications toward highly efficient nitroarene reduction reactions. We prepared the catalyst through a co-reduction of potassium tetrachloroplatinate (II) and palladium chloride (II) in polyvinylpyrrolidone, with subsequent deposition on commercially available Fe_3O_4 nanoparticles. After immobilization of the transition metals, we utilized the nanocatalysts for the efficient reduction on a variety of nitro-compounds, and all the reactions examined proceeded with high yields and chemoselectivities in 5 min. Furthermore, the spent catalysts could be recovered and reused up to 250 times without any loss of catalytic activity.

Key words: bimetallic nanocatalyst, heterogeneous catalyst, magnetically recyclable catalyst nitro reduction, selectivity, synergestic effect

***Student number*: 2014-25133**

List of Figures

List of Schemes

List of Tables

Synthesis of Pd–Pt–Fe_3O_4 nanoflakes and their performance as magnetically recyclable catalysts for nitroarene reduction

I. Introduction

During the last decade, new types of nanoparticles have been continuously developed to furnish desirable catalytic properties.[1-3] Numerous novel nanoparticles with unique physical (optical,[4] structural,[5] electronic,[6] and magnetic[7]) properties have been documented. Especially, significant attention has been paid to the development of bimetallic nanomaterials,[8,9] including bimetallic nanoparticles. These bimetallic nanoparticles have been at the center of interests for many applications because of their extraordinary chemical activities that are different from those of the parent metals.[10-12]

Among the nanoparticles, significant research has been conducted on magnetically recoverable nanoparticles for their scientific, technological, and industrial importance as excellent durable catalysts.[13-18] Magnetic nanoparticles have many advantages including their facile recovery from reaction media through the use of an external magnet. This approach significantly enhances the efficiency of these catalysts, offering great potential for industrial applications. Hence, new types of heterogeneous catalysts and reactions based on magnetic separation have been extensively developed because of their merits. Thus, further enhancement of their catalytic performance, utilization efficiency, and recyclability continues to be a significant issue.

Reduction of nitro compounds is one of the most fundamental reactions in organic synthesis. It is also one of the most essential methods for the preparation of functionalized aromatic amines, which are ubiquitously found in pharmaceuticals,[19] natural products,[20] pigments,[21] and polymers.[22] Consequently, various metal catalysts based on Pd,[23,24] Pt,[25-27] Au, [28-30] Fe, [31,32] Co[33] and Ni[34] have been employed for their preparation. The use of catalytic reduction conditions[35] employing metal-catalyzed hydrogenation with advanced methodologies have been significantly developed because of its atom efficiency, compatibility with industrial applications, and eco-

friendliness. Sustainable processes for the reduction of substituted nitro compounds require highly active catalysts for chemoselective reaction. Alcohols such as isopropanol,[36] glycerol,[37] and ethanol[38] have been utilized as hydrogen providers. However, reductions using these hydrogen sources typically exhibit low selectivity and slow reaction rates. Recently, ammonia borane has become an attractive hydrogen carrier for hydrogenation because of its nontoxicity, high volume/mass hydrogen density, good solubility in water and alcoholic solvents and facile release of H_2 through hydrolysis of water and alcoholysis of alcohols.[39, 40] In particular, it has gained wide popularity for the reduction of double bonds, carbonyls, imines, nitriles, and nitro compounds under ambient conditions in aqueous solutions.[41]

Previously, we have been interested in using efficient catalysts based on magnetically recyclable iron oxide nanaoparticles for useful synthetic organic applications. In our laboratory, we reported the synthesis and catalytic applications of novel nanoparticles such as Rh–Fe_3O_4 and Pd–Fe_3O_4[42-48].

Here we report a highly efficient and magnetically recyclable catalytic system using Pd–Pt–Fe_3O_4, and its performance on reducing nitroarenes. The bimetallic Pd–Pt–Fe_3O_4 nanoparticles were easily prepared via a solution phase hydrothermal method on a multi-gram scale and exhibited unique surface textures and morphologies. The nanocatalysts provided a unique synergistic effect for the catalysis of cascade dehydrogenation/reduction. Excellent yields of the desired products were obtained within 5 min, with long-term recyclability of the catalyst. This efficient, recyclable Pd–Pt–Fe_3O_4 nanoparticle system can therefore be repetitively utilized for the reduction of various nitro-containing compounds.

II. Result and Discussion

The bimetallic Pd–Pt–Fe_3O_4 nanoparticles were easily prepared using a facile one-pot solution phase hydrothermal method involving the co-reduction of palladium chloride (II) and potassium tetrachloroplatinate (II) in polyvinylpyrrolidone (PVP) and ethylene glycol (EG), followed by deposition of the two transition metals on commercially available Fe_3O_4 nanocrystals. Reduction of 1.92 mmol each of $PdCl_2$ and K_2PtCl_4 was carried out, resulting in a Pd:Pt molar ratio of nearly 1.0:1.0. PVP served as a dispersant[49] and sterically stabilized the nanoparticles,[50] whereas EG functioned as both the solvent and a reductant. Inductively coupled plasma-atomic emission spectroscopic (ICP-AES) analysis indicated that the nanocatalysts contained 5.1 wt% palladium and 8.3 wt% platinum. The bimetallic Pd–Pt–Fe_3O_4 nanoparticles have diameters of approximately 90 to 180 nm. **Figure 1** illustrates representative HRTEM and SEM-EDS images of the nanoflake Pd–Pt–Fe_3O_4 NPs. These images show the surfaces of the nanoflaked-shaped nanoparticles, with well-dispersed metals having diameters ranging from 5 to 8 nm. Through the mapping image of the **Figure 1b**, we can see that the surface of the Fe_3O_4 support (yellow) is nearly evenly loaded with Pd (red) and Pt (blue).

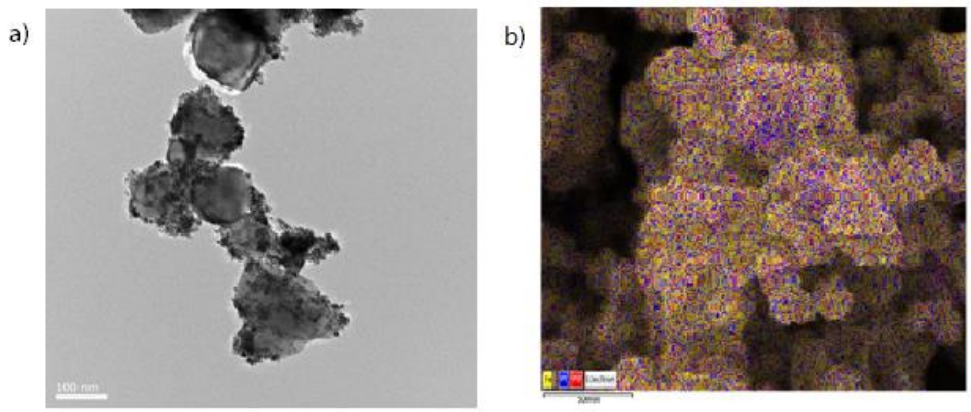

Figure 1. a) HRTEM and b) SEM-EDS images of the Pd–Pt–Fe_3O_4 nanoparticles.

It became evident that the two metal nanoparticles exist in an alloy form for our present catalyst. Cs-STEM images and Cs-STEM-EDS mapping images of the **Figure 2** confirmed the alloy dispersion Pd and Pt nanoparticles on Fe_3O_4. As shown on the **Figure 2a and 2b**, metals are forming together sphere shapes, and **Figure 2c and 2d** detail the dispersion of Pt and Pd on the surface by color detection. The mixture of colors proves that there is Pd–Pt bimetallic alloy on the surface of the nanoparticle catalyst.

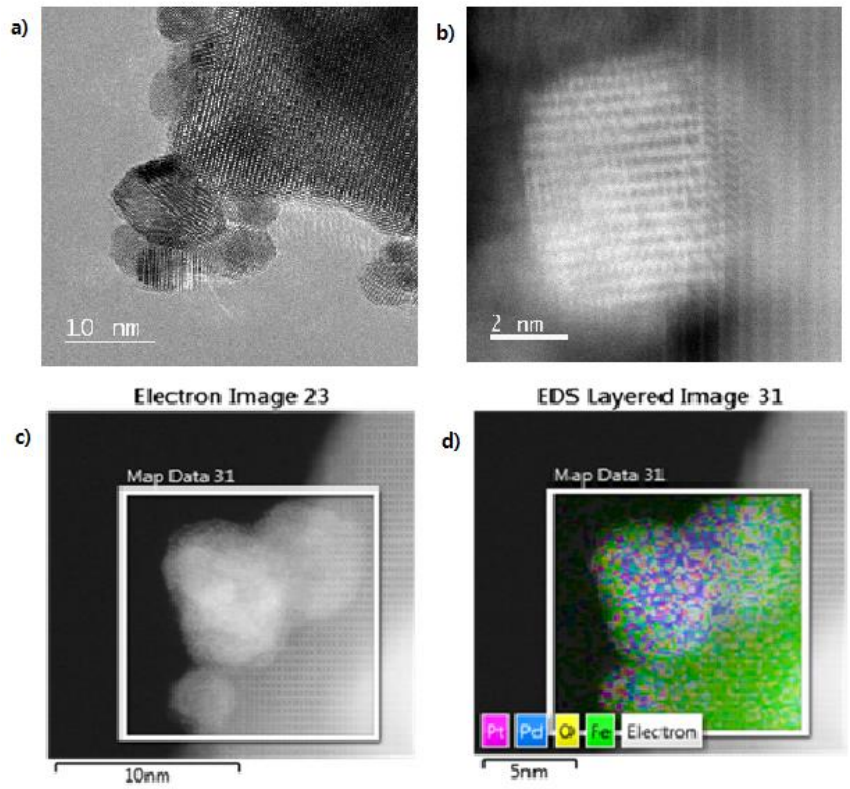

Figure 2. a) and b) Cs-STEM images of Pd–Pt–Fe_3O_4, c) and d) Cs-STEM-EDS images of Pd–Pt–Fe_3O_4.

X-ray diffraction (XRD) patterns were also analyzed to check the presence of alloy dispersion. The formation of alloy is detectable by a change in lattice peaks when compared with the monometallic one.[51] Therefore, we compared the X-ray diffraction (XRD) patterns of mono metallic catalysts (Pd and Pt–

Fe_3O_4) and bimetallic Pd–Pt–Fe_3O_4 nanoparticles as given in **Figure 3.** A subtle difference in lattice peaks was observed, confirming again the bimetallic alloy dispersion of Pd and Pt nanoparticles on Fe_3O_4.

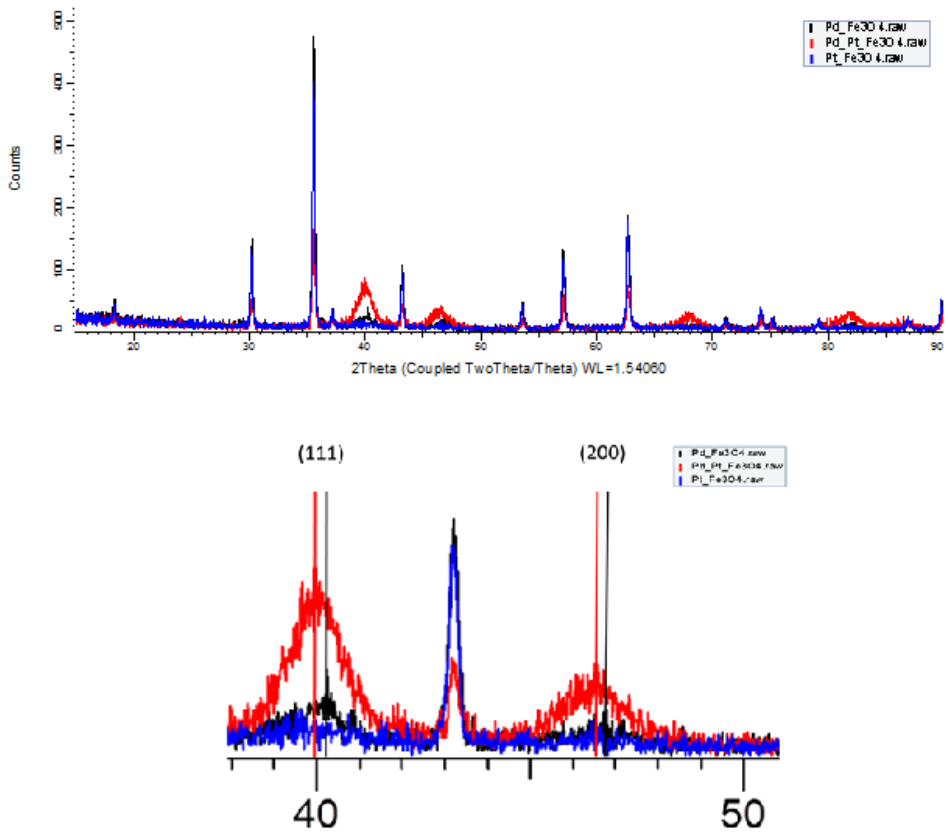

Figure 3. XRD data of Pd– Fe_3O_4, Pt–Fe_3O_4, Pd–Pt–Fe_3O_4

The oxidation states of the metals were determined by X-ray photoelectron spectroscopy (**Figure 3**). Two characteristic Pt $4f_{7/2}$ and Pt $4f_{5/2}$ peaks indicated the presence of Pt(0) species (**Figure 3a**).[52] In the same way, the characteristic peaks Pd $3d_{5/2}$ and Pd $3d_{3/2}$ revealed that Pd(0) was present in the nanocatalyst (**Figure 3b**).

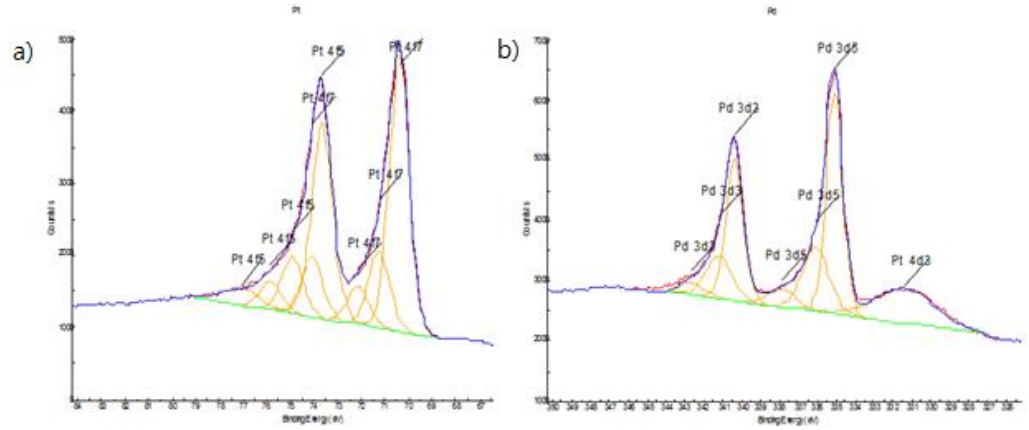

Figure 4**. XPS spectrum of a) Pt 4f, b) Pd 4d.**

To complete the characterization of the bimetallic Pd–Pt–Fe_3O_4 nanoparticles, we carried out an analysis of their magnetic properties. Magnetic property measurement system (MPMS) data clearly indicated that the Pd–Pt–Fe_3O_4 nanaoparticles, whose saturation magnetization value was 58.4 emu g−1 (Fe) at 300 K, were superparamagnetic (**Figure 4**).

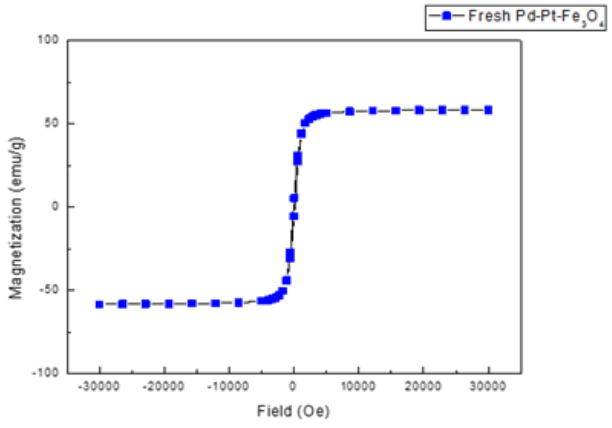

Figure 5. MPMS data of Pd-Pt- Fe_3O_4 nanoparticles.

The application of the Pd–Pt–Fe_3O_4 nanoparticles on organic reactions began with screening various parameters on nitrobenzene reduction, with ammonia-borane as hydrogen source. The results are summarized in **Table 1**.

Table 1. Optimization of nitro reduction by Pd–Pt–Fe_3O_4

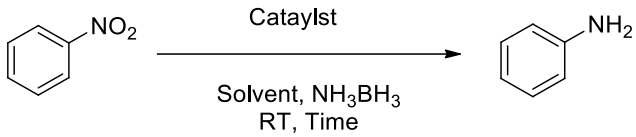

Entry	Catalyst	Solvent	Time	Yield[b]	Conversion[b]
1	None	MeOH	5 min	0	0
2	Fe_3O_4	MeOH	5 min	0	0
3	1 mol% Pd–Fe_3O_4	MeOH	5 min	40	68
4	1 mol% Pt–Fe_3O_4	MeOH	5 min	56	69
5[c]	1 mol% Pd–Fe_3O_4 & Pt–Fe_3O_4	MeOH	5 min	57	90
6	1 mol% Pd–Pt–Fe_3O_4	MeOH	5 min	>99	>99
7	1 mol% Pd–Pt–Fe_3O_4	H_2O	5 min	84	93
8	1 mol% Pd–Pt–Fe_3O_4	EtOH	5 min	64	75
9[d]	1 mol% Pd–Pt–Fe_3O_4	H_2O:EtOH	5 min	>99	>99
10[d]	1 mol% Pd–Pt–Fe_3O_4	H_2O:MeOH	5 min	>99	>99
11	0.1 mol% Pd–Pt–Fe_3O_4	MeOH	30 min	>99	>99
12	0.01 mol% Pd–Pt–Fe_3O_4	MeOH	3 h	>99	>99
13	0.001 mol% Pd–P–Fe_3O_4	MeOH	30 h	>99	>99
14[e]	1 mol% Pd–Pt–Fe_3O_4	MeOH	5 min	>99	>99

[a] Reaction conditions: 0.5 mmol nitrobenzene, 1.5 mmol NH_3BH_3, 5 mL solvent, and room temperature. [b] Yields and conversions were determined via GC analysis using anisole as an internal standard. [c] 1 mol% of each catalyst. [d] 5 mL of water/solvent (v/v=3:7). [e] 10 mmol nitrobenzene.

First, we tested a series of catalysts. Reactions carried out with no catalyst or with Fe_3O_4 nanoparticles didn't give the desired product (0% Yield, **Table 1, Entries 1 and 2**). The reactions were then performed with various Fe_3O_4-based nanoparticles catalysts (**Table 1, Entries 3–6**). The Pd–Pt–Fe_3O_4 nanoparticles exhibited the best catalytic activity in methanol, furnishing the highest conversion (>99%) and yield (>99%) (**Table 1, Entry 6**). Furthermore, the comparison of the reaction employing Pd–Pt–Fe_3O_4 catalysts with that of monometallic catalysts (**Table 1, Entries 3 and 4**) or physical combination of the two (**Table 1, Entry 5**) revealed a distinctive synergistic effect.[53] This effect can be attributed to the fact that Pd and Pt atoms are located near each other in an alloy form in the nanoparticles, as described previously by the mapping images. Next, different solvents were tested. The conversion and yield decreased when the reaction was conducted in water or ethanol (**Table 1, Entries 7 and 8**). Using binary solvent systems such as water–ethanol (v/v 3:7) or water–methanol (v/v 3:7) improved the reaction efficiency (**Table 1, Entries 9 and 10**). In fact, the reduction reaction occurs apparently through hydrolysis of water or alcoholysis. However, nitrobenzene has a better solubility in an alcoholic solvent, which explains the promising results of reactions carried out in a mixture of water and alcohol.

Furthermore, the reactions were tested with reduced Pd–Pt–Fe_3O_4 catalyst loading (0.1, 0.01, and 0.001 mol %) and effective results could be obtained through elongation of reaction times (1, 3, and 30 h for **Table 1, Entries 11-13,** respectively). A larger scale (10 mmol) reaction was also successfully performed giving >99% yield (**Table 1,** entry 14), warranting potential industrial-scale applications.

Different reducing agents were also tested, as shown in **Table 2**. When hydrazine[53] or 1,1,3,3,-tetramethyldisiloxane[54] was used as a hydrogen source, poor yield was obtained over 5 min of reaction time (**Table 2, Entries 1 and 2**). Bubbling hydrogen led to complete reaction in 5 min, however, reaction under atmospheric hydrogen was slow (1 h) (**Table 2, Entries 4 and 5**) .

Table 2. Variation of reducing agent[a]

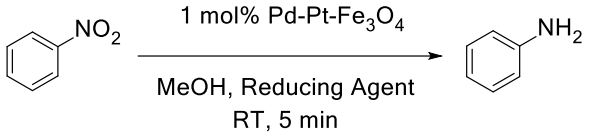

Entry	Reducing Agent	Yield (%)[b]	Conversion (%)[b]
1	Hydrazine	0	0
2	1,1,3,3- Tetramethyldisiloxane	0	0
3	NH_3BH_3	>99	100
4[c]	H_2 (1 atm)	>99	100
5	H_2 (bubbling)	>99	100

[a] Reaction conditions: 0.5 mmol substrate, 1.5 mmol reduciong agent, 1 mol% Pd-Pt-Fe_3O_4 catalyst, 5mL of solvent and room temperature. [b] Yields and conversions were determined from GC analysis using anisole as an internal standard. [c] Reaction time (1 h).

To establish the substrate scope for the nitro reduction in presence of the bimetallic Pd–Pt–Fe_3O_4 nanoparticles, we have screened an array of nitro compounds. As summarized in **Table 3**, high yields and conversions were obtained for all the compounds examined within a fast reaction time in methanol. Very specific chemoselectivity was observed for nitroarene derivatives having halide functional groups without dehalogenation reaction (**Table 3, Entries 2−4**). The reaction proceeded highly efficiently for substrates containg both electron-donating groups (**Table 3, Entries 5-9**) and an electron-withdrawing substituent (**Table 3, Entry 10**). We also tested the catalytic reaction for 1-nitronaphthalene, 4-nitrobiphenyl, and 2,7-dinitrofluorene, which furnished desired products in excellent yields (**Entries 12, 13, and 14**).

Table 3. Substrate scope for reduction of nitro compounds[a]

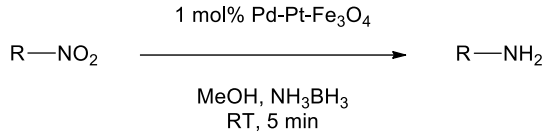

Entry	Substrate	Product	Yield (%)[b]	Conversion (%)[b]
1	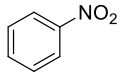	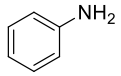	>99 (96)	>99
2	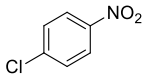	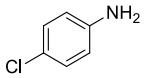	98 (93)	>99
3	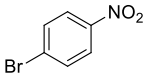	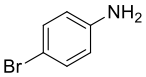	>99 (91)	>99
4	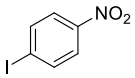	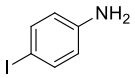	>99 (95)	>99
5	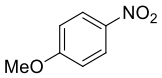	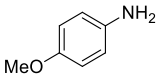	98 (94)	>99
6	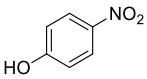	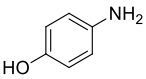	>99 (93)	>99
7	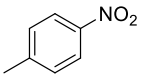	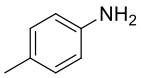	>99 (93)	>99
8	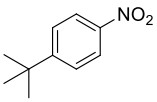	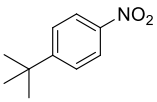	>99 (92)	>99
9	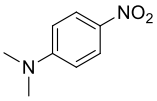	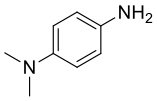	98 (90)	>99
10	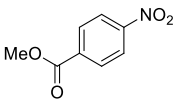	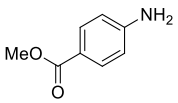	98 (97)	>99
11	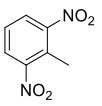	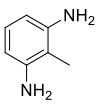	>99 (95)	>99

12	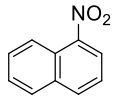	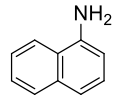	>99 (98)	>99
13	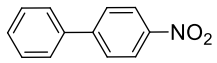	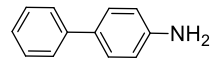	>99 (97)	>99
14[c]	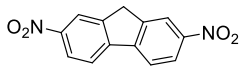	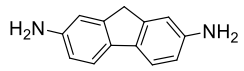	>99 (97)	>99
15	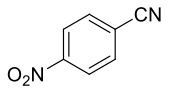	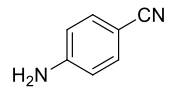	>99 (96)	>99
16	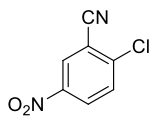	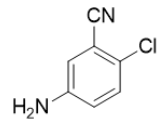	>99 (92)	>99
17	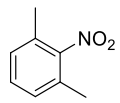	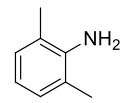	>99 (93)	>99
18[d]	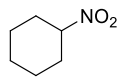	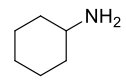	>99 (94)	>99
19	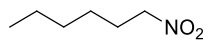	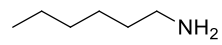	>99 (95)	>99

[a] Reaction conditions: 0.5 mmol substrate, 1.5 mmol NH_3BH_3, 1 mol% Pd–Pt–Fe_3O_4 catalyst, 5 mL methanol, room temperature. [b] Yields were determined via GC analysis using anisole as an internal standard. Numbers in parentheses are isolated yields. [c] Reaction time was 30 min.

These heteroaromatic amine derivatives are important intermediates for the production of drug molecules, insecticidal/antimicrobial agents, dyes, and recently compounds used in organic displays.[55]

Reactions with nitrile-containing compounds revealed the chemoselectivity for nitro-reduction over nitrile reduction (**Table 3, Entries 15 and 16**). A sterically hindered substrate was also reduced to the corresponding aniline

product (**Table 3, Entry 17**). Finally, aliphatic nitro substrates furnished the desired products efficiently (**Table 3, Entries 18 and 19**).

Additional chemoselectivity studies were carried out through the reduction of 4-nitrostyrene (**Table 4**).

Table 4. Chemoselectivity studies of 4-nitrostyrene reduction[a]

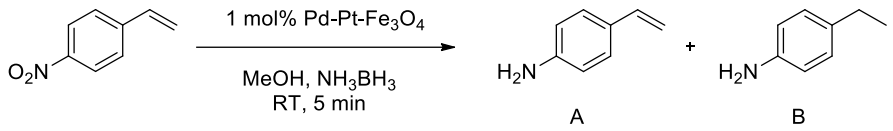

Entry	Equivalent of NH_3BH_3	Conversion (%)[b]	Selectivity (A:B)[b]
1	3 eq	> 99	0:100
2	1 eq	> 99	94:6

[a] Reaction conditions: 0.5 mmol substrate, 1mol% Pd-Pt-Fe_3O_4 catalyst, 5 mL methanol and room temperature. [b] Yields were determined by GC analysis using anisole as internal standard.

Under the identical reaction conditions using 3 equiv ammonia borane, both nitro and olefin moieties of 4-nitrostyrene were reduced, giving the product **B**. However, when 1equiv ammonia borane was used, we obtained the desired product **A** with a small amount of the fully reduced product **B**, (A/B = 94:6).

With the same procedure, we studied the selectivity of aromatic nitro groups in presence of various alcohol protecting groups (**Table 5**).

Table 5. Selectivity studies of protected nitro compounds and nitroacetophenone[a]

Entry	Substrate	Product	Isolated Yield (%)
1	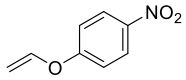	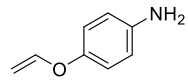	93
2	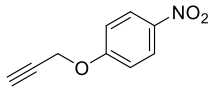	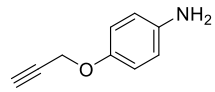	92
3[b]	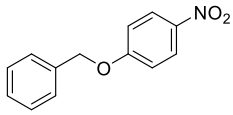	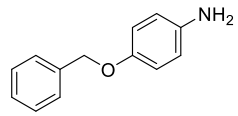	93
4[c]	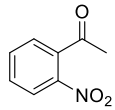	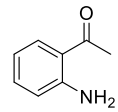	97

[a] Reaction conditions: 1 mmol substrate, 1 mmol NH_3BH_3, 1 mol% Pd–Pt–Fe_3O_4 catalyst, 10 mL methanol, room temperature. [b] 1,5 mmol NH_3BH_3, 10 min. [c] 3 mmol NH_3BH_3, 5min of reaction time.

When nitro compounds containing *O*-allyl, *O*-propargyl groups were tested, *O*-allyl or *O*-propargyl protected nitrobenzene was selectively reduced to the corresponding aniline derivatives, respectively (**Table 5, Entries 1 and 2**). When the reduction of 1-benzyloxy-4-nitrobenzene was performed with 1.5 equiv ammonia borane for 10 min at room temperature, the desired product was obtained in 93% yield **(Table 5, Entry 3)**. We also evaluated the selectivity on the reduction of *o*-nitroacetophenone (**Table 5, Entry 4**). The reduction of the nitro group on *o*-nitroacetophenone was highly efficient without the undesired ketone reduction. Through the studies summarized in **Tables 4 and 5**, we were able to achieve a chemoselective reduction of nitro

compounds using Pd–Pt–Fe_3O_4 nanoparticles by controlling the reducing agent stoichiometry.

Table 6. Chemoselectivity studies of *o*-nitrobenzaldehyde

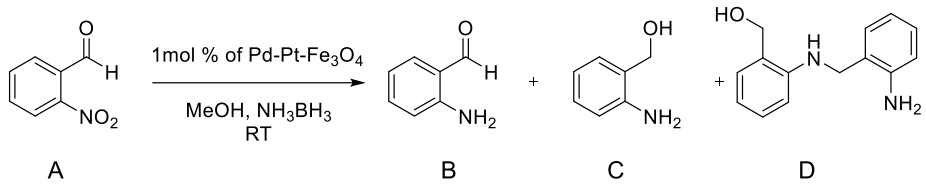

A B C D

Entry	Eq of AB	Reaction time	Yield of B[b]	Yield of C[b]	Yield of D[b]
1	3	5 min	0%	95%	0%
2	1	5 min	0%	49%	48%

[a] Reaction conditions: 1 mmol substrate, 1 mol% Pd–Pt–Fe_3O_4 catalyst, 10 mL methanol, room temperature. [b] Yield of isolated products

The last case of selectivity studies concerned the reduction of *o*-nitrobenzaldehyde (**Table 6)**. When the reaction was carried out with 3 equiv ammonia borane (**Table 6, Entry 1**), both nitro and aldehyde groups were reduced, giving the fully reduced nitrobenzyl alcohol as a major product **C** (95%). Then, we decided to test the same reaction by decreasing the amount of ammonia borane to 1 equiv (**Table 6, Entry 2**). For this case, the product **C** and the dimerization product **D** were obtained, with a ratio of 1:1.

The mechanism of the nitro reduction catalyzed by the Pd–Pt–Fe_3O_4 nanoparticles is described in **Scheme 1**. The mechanism describes a tandem reaction involving the nitro reduction and the methanolysis of ammonia borane used as a hydrogen source. The reaction was postulated to undergo through nitrosobenzene and diazobenzene as depicted in **Scheme 1**, and the presence of the presumed reaction intermediates such as nitrosobenzene and azobenzene was confirmed through gas chromatography mass spectrometry, as shown in **Figure 6**.

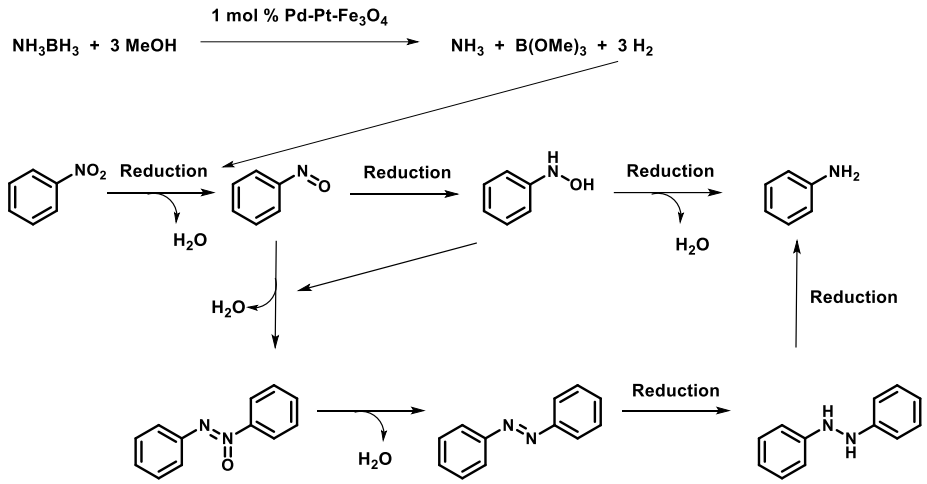

Scheme 1. Proposed mechanism of nitro reduction catalyzed by Pd–Pt–Fe_3O_4

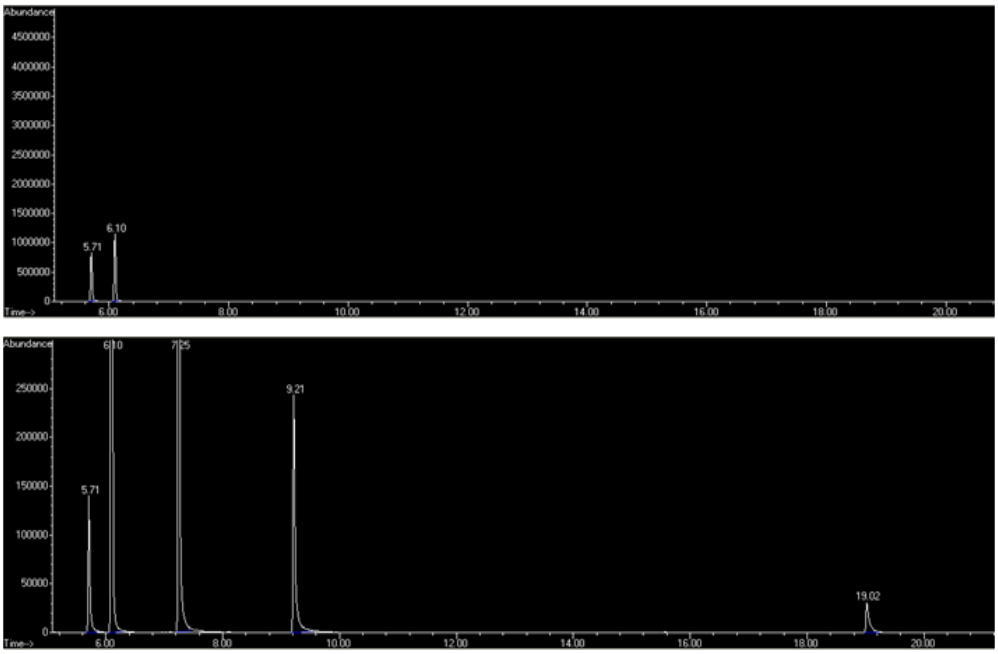

Figure 6. (a) GC-MS data of the commercially available nitrosobenzene and anisole (b) GC-MS data of the nitrobenzene reduction after 3 min of reaction

The **Figure 6a** shows the GC spectrum of the commercially available nitrosobenzene (5.71 min) and anisole (6.10 min) used as internal standard. Nitrobenzene reduction reaction was also analyzed by GC-MS (**Figure 6b**). The presence of nitrosobenzene was checked by the same retention time with the commercially available one (5.71 min). The other detected peaks correspond to aniline (7.25 min), nitrobenzene (9.21 min) and azobenzene (19,02 min) which represents another intermediate of the reaction.

Recyclability of the Pd–Pt–Fe_3O_4 nanoparticle catalyst was investigated. When the reduction of nitrobenzene was completed under the normal reaction condition, the nanoparticles could be easily separated from the reaction mixture through the use of an external magnet (**Figure 7**).

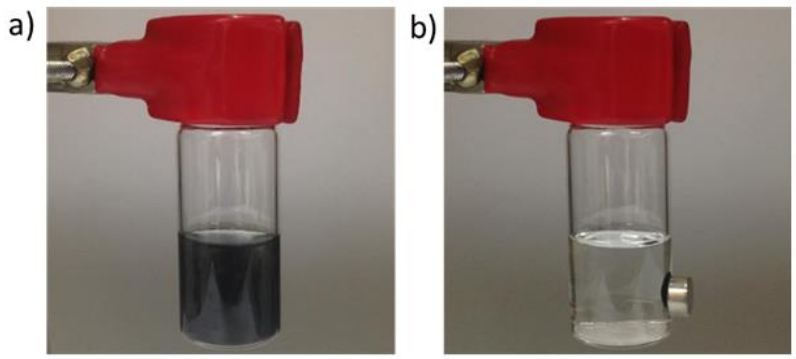

Figure 7. Photographs of the magnetically separable Pd–Pt–Fe_3O_4: a) dispersion state, b) magnetic separation after reaction

Then, a new catalytic reduction cycle could be repeated with the recovered catalyst, with fresh substrate and ammonia borane. As described in **Figure 8**, the catalyst showed excellent catalytic performance until 250 cycles.

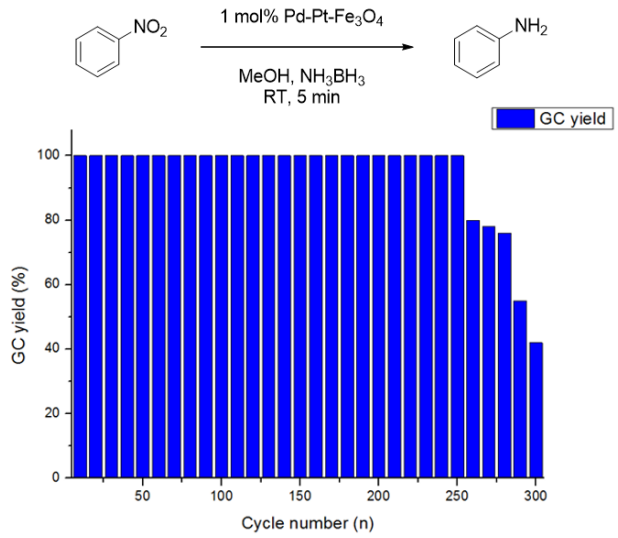

Figure 8. Recycling Test of the Pd–Pt–Fe_3O_4 nanoflake catalyst

To understand the decreased activity after 250 cycles, we first employed thermogravimetric analysis (TGA), ICP-MS (**Table 7**) and Fourier transform infrared spectroscopy (IR) (**Figure 9**) to investigate the difference bewteen the fresh catalyst and recycled (spent) Pd–Pt–Fe_3O_4 nanoparticles. These analyses revealed that the composition of the catalyst remained nearly identical upon recycling, explaining the continuous excellent catalytic activity of the Pd–Pt–Fe_3O_4 nanoparticles until 250 cycles.

Table 7. The weight percent of elements through ICP-MS

Cycle number (n)	Pd (wt%)	Pt (wt%)
0 (Fresh)	5.1	8.3
10	5.0	8.1
30	5.1	8.2
300	5.0	8.0

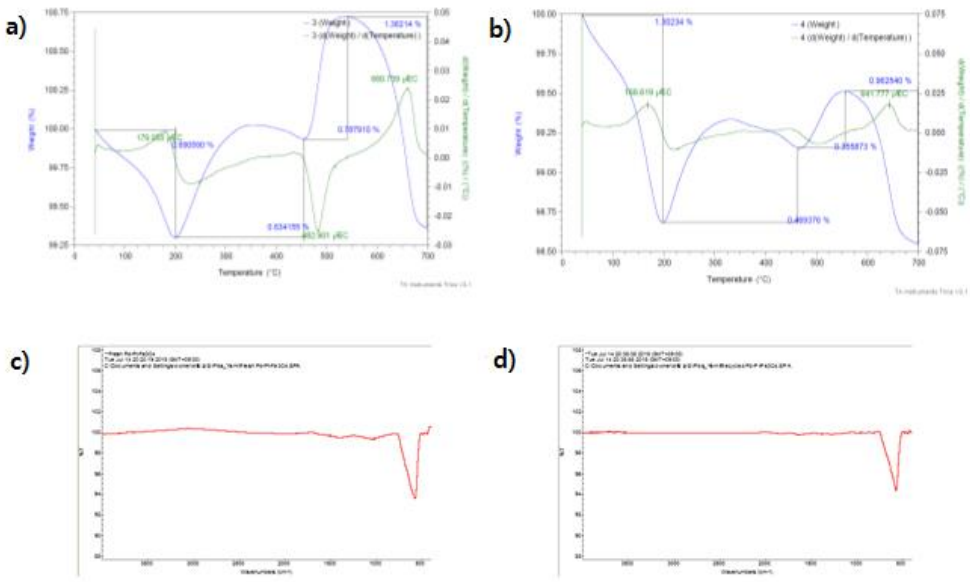

Figure 9. a) TGA of the fresh catalyst, b) TGA of the spent catalyst, c) IR of fresh catalyst, d) IR of spent catalyst

We also carried out analyses of the catlaysts through High Resolution Transmission Electron Microscopy (HRTEM) and Scanning Electron Microscope (SEM) (**Figure 10**). **Figure 10a and 10c** show HRTEM and SEM images of the fresh Pd–Pt–Fe_3O_4 nanoflakes, with well-dispersed Pd and Pt nanoparticles. The HRTEM and SEM data of the spent catalyst after 300th cycle of catalytic reactions revealed changes in the physical properties of the catalyst. Agglomeration[56] of the loaded Pd and Pt nanoparticles was visible (**Figure 10b and d**). This data indicated that the reduction in catalytic activity was probably due to the agglomeration of Pd and Pt nanoparticles on the surface of Fe_3O_4, rather than detachment[57] from the support.

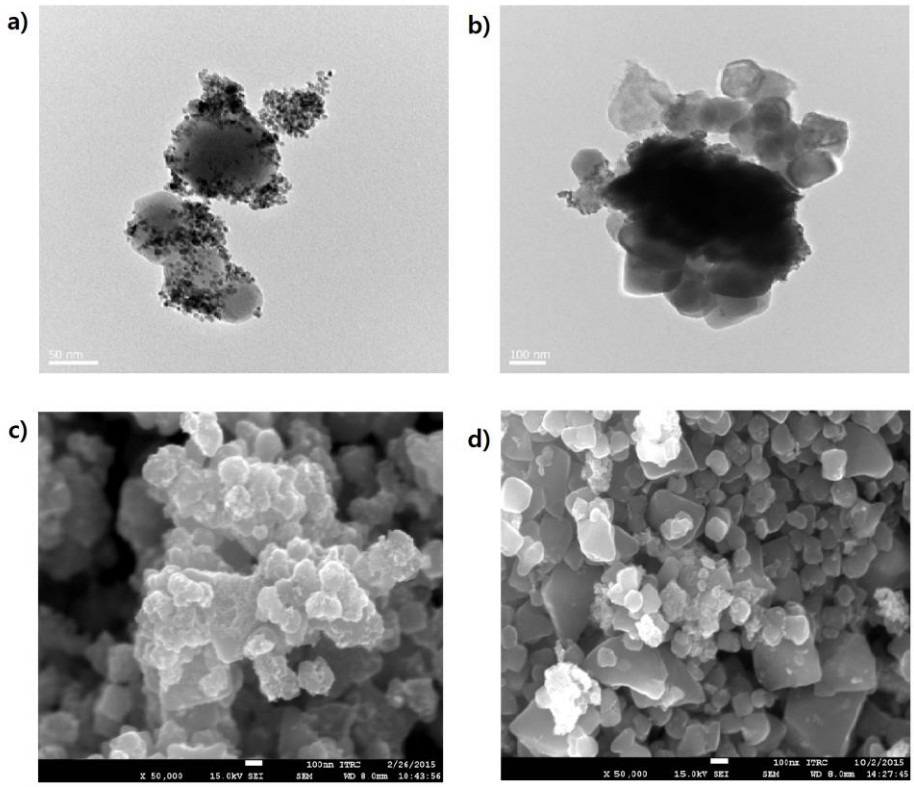

ys t after 300 cycle of catalytic reactions, c) SEM of fresh catalyst, d) SEM of spent catalyst after 300 cycle of catalytic reactions

III. Conclusion

In Summary, we have investigated a new catalytic system for the reduction of nitro compounds. Bimetallic nanoflake-shaped Pd–Pt–Fe_3O_4 nanoparticles were synthetized through a simple hydrothermal method. The performance of the catalyst on the dehydrogenation of ammonia borane and reduction of various nitro compounds was highly efficient, giving excellent conversions and yields in only 5 min at room temperature. Moreover, the presence of bimetallic Pd and Pt alloy was a key element to explain the synergistic effect that our catalyst provided. Chemoselectivitiy studies revealed nitro-groups were selectively reduced without affecting protecting groups or other functional groups such as allyl, propargyl or ketone groups. The bimetallic Pd–Pt–Fe_3O_4 nanoparticles were effective at a low loading level, and showed also great applicability for large-scale reactions. Finally, having Fe_3O_4 as support, Pd–Pt–Fe_3O_4 nanoparticles were applied as magnetically separable catalysts. The catalyst was easily recovered and reused 250 times without loss of catalytic activity. Therefore, bimtallic Pd–Pt–Fe_3O_4 nanoparticles are good candidates as catalysts with easy recovery and excellent efficiency, offering possibly an environmentally friendly solution for industial applications[75].

IV. Experimental

Materials

All chemicals were commercially available and used as received without further purification. Potassium platinochloride (98% purity), palladium chloride (99% purity) and polyvinylpyrrolidone (PVP) were purchased from Sigma-Aldrich. Iron oxide was purchased from Skyspring nanomaterials.

Characterization methods

All reaction products were identified through comparison with authentic compounds and quantified through gas chromatography/mass spectrometry (GC-Mass) analysis using a Hewlett Packard 5890 Gas Chromatograph with anisole as an internal standard. All Transmission Electron Microscopy (TEM) images were obtained on a JEOL EM-2010 microscope at an accelerating voltage of 200 kV. The powder X-ray diffraction (XRD) was performed using a Bruker AXS D8 FOCUS (2 theta: 5-100, scan speed: 2degree/min, Cu Kαradiation: λ=1.54056nm, Generator: 40kV, 40m). Measurement of magnetic properties of catalysts was performed through Magnetic Property Measurement System (MPMS) from Quantum Design. The energy disperse spectroscopy (EDS) map sum spectrum pattern was performed using an Oxford Instruments X-Maxn (software: Aztex). Sonication was performed in a 120 W ultrasonic bath (Branson, B-3210) and Sonics & Vibra cell VCX 750. Fourier transform infrared (FTIR) spectra were recorded on a Nicolet iS10 spectrometer through the use of KBr pellets. Thermogravimetric analysis (TGA) was performed on a TGA Q5000 V3.10 Build 258 instrument at a heating rate of 10 °C min^{-1} under a nitrogen flow.

Synthesis of the Pd–Pt–Fe_3O_4

The synthesis of Pd-Pt-Fe_3O_4 was performed as follows. First 800 mg of potassium platinochloride (K_2PtCl_4), 340 mg of palladium(II) chloride ($PdCl_2$) and 1.00 g of polyvinylpyrrolidone (PVP) (Mw ~10,000) were dissolved in 80 mL of ethylene glycol (EG) in a 250 mL round-bottom flask. This mixture was sonicated for 10 min and heated at 100°C for 1 h in oil bath with magnetic stirring. Meanwhile, 1.00 g of Fe_3O_4 was dissolved in 300 mL of EG in a two-necked 500 mL round-bottom flask and then ultrasonication performed for 40 min. Next, with vigorous stirring of the Fe_3O_4 solution with a mechanical stirrer, the prepared platinum and palladium precursor solution was injected dropwise. The resulting solution was further processed at 100 °C for an additional 24 h. Afterward, the resultant sample could be retrieved via centrifugation and washing with absolute ethanol. Finally, the product was obtained via drying on a rotary evaporator.

General procedure for the catalytic cascade reduction reaction

The nanoflake-shaped Pd-Pt-Fe_3O_4 catalyst (1.00 mol %), R-NO_2 (0.500 mmol), anisole (internal standard, 0.500 mmol) and methanol (5.0 mL) were introduced in a glass vial (10 mL) with a magnetic stirrer bar. The mixture was sonicated for 1 min and stirred at room temperature for 5 min. Then, the ammonia-borane complex (1.50 mmol) was added to the reaction mixture, and the vessel was closed with a Teflon cover. This reaction was vigorously stirred for 5 min at room temperature. After completion of the reaction, an aliquot from the organic layer was analyzed with gas chromatography. The separation of the catalyst was realized with a small magnet from outside of the vial. The remaining catalyst was washed three times with methanol. The solvent was then removed with the use of a rotary evaporator, therefore allowing the dried catalyst to be reused for a further recycling reaction.

General procedure for the recycling the Pd–Pt–Fe_3O_4

For the recycling test, the reduction of nitrobenzene was scaled up to 1.00 mmol and reductions were run using 1 mol% catalyst. Each reaction cycle was complete within 5 min at room temperature. After each reaction, the catalyst was separated with a magnet and washed with methanol. Nitrobenzene (1.00 mmol), anisole (1.00 mmol) and methanol (10 mL) were then added directly to the washed catalyst. Then the reaction was performed by applying the general procedure for the nitro-reduction reaction. The catalytic reactions were then repeated during 10 cycles. Each cycle was analyzed by gas chromatography mass spectrometry (GC-Mass)

Chemical studies

^{1}H and ^{13}C NMR spectra were acquired through the Agilent MR DD2 (400 MHz) spectrophotometer. The signals were reported as s (singlet), d (doublet), t (triplet), q (quartet), m (multiplet and chemical shifts were measured as parts per million (δ values) from tetramethylsilane as an internal standard at probe temperature in $CDCl_3$ or DMSO-D_6.

Aniline (Table 2, Entry 1)[58]

^{1}H-NMR (400 MHz, $CDCl_3$) δ: 7.16 (m, 2H), 6.77 (m, 1H), 6.69 (m, 2H), 3.35 (s, 2H). ^{13}C-NMR (100 MHz, $CDCl_3$) δ: 146.41, 129.41, 118.73, 115.26.

Amino-4-chlorobenzene (Table 2, Entry 2)[59]

^{1}H-NMR (400 MHz, $CDCl_3$) δ: 7.08 (d, J = 8.4 Hz, 2 H), 6.58 (d, J = 8.8 Hz, 2 H), 3.63 (s, 2H). ^{13}C-NMR (100 MHz, $CDCl_3$) δ: 144.90, 129.05, 123.05, 116.17.

Amino-4-bromobenzene (Table 2, Entry 3)[60]

^{1}H-NMR (400 MHz, $CDCl_3$) *δ:* 7.24 (d, *J*=8.72 Hz, 2 H), 6.55 (d, *J*=8.72 Hz, 2 H), 3.67 (s, 2 H). ^{13}C-NMR (100 MHz, $CDCl_3$) *δ*: 146.0, 131.8, 117.1, 109.0.

4-Iodoaniline (Table 2, Entry 4)[61]

^{1}H-NMR (400 MHz, $CDCl_3$) δ: 7.44 (d, *J*=8.6 Hz, 2H), 6.48 (d, *J*=8.6 Hz, 2H), 3.69 (s, 2H, NH). ^{13}C-NMR (100 MHz, $CDCl_3$) δ: 79.6, 117.5, 138.1, 146.3.

4-Methoxyaniline (Table 2, Entry 5)[62]

^{1}H-NMR (400 MHz, $CDCl_3$) δ: 6.75 (d, J = 8.9 Hz, 2H), 6.65 (d, J = 8.9 Hz, 2H), 3.75 (s, 3H), 3.41 (s, 2H, NH). ^{13}C-NMR (100 MHz, $CDCl_3$) δ: 152.9, 140.0, 116.6, 114.9, 55.9.

4-Aminophenol (Table 2, Entry 6)[58]

^{1}H-NMR (400 MHz, DMSO-d6) δ: 6.45 (d, J = 8.56 Hz, 2H), 6.38 (d, J = 8.56 Hz, 2H), 4.35 (s, 2H). ^{13}C-NMR (100 MHz, DMSO-d6) δ: 149.10, 141.12, 115.98, 115.66 .

***p*-Toluidine (Table 2, Entry 7)[62]**

^{1}H-NMR (400 MHz, $CDCl_3$) δ: 6.99 (d, J = 8.3 Hz, 2H), 6.63 (d, J = 8.3 Hz, 2H), 3.53 (s, 2H, NH), 2.26 (s, 3H). ^{13}C-NMR (100 MHz, $CDCl_3$) δ: 143.9, 129.9, 127.9, 115.4, 20.6.

4-*tert*-Butylaniline (Table 2, Entry 8)[59]

^{1}H-NMR (400 MHz, $CDCl_3$) δ: 7.05 (d, J = 8.4 Hz, 2 H), 6.55 (d, J = 8.8 Hz, 2 H), 3.44 (s, 2H), 1.20 (s, 9H). ^{13}C-NMR (100 MHz, $CDCl_3$) δ: 143.74, 141.32, 125.98, 114.86, 33.85, 31.49.

***N,N*-Dimethyl-*p*-phenylenediamine (Table 2, Entry 9)[63]**

^{1}H-NMR (400 MHz, $CDCl_3$) δ: 6.71 – 6.64 (m, 4H), 3.19 (s, 2H), 2.82 (s, 6H). ^{13}C-NMR (100 MHz, $CDCl_3$) δ: 144.7, 138.0, 116.5, 115.5, 42.0.

Methyl 4-aminobenzoate (Table 2, Entry 10)[62]

^{1}H-NMR (400 MHz, $CDCl_3$) δ: 7.84 (d, J = 8.1 Hz, 2H), 6.63 (d, J = 8.1 Hz, 2H), 4.05 (s, 2H, NH), 3.85 (s, 3H). ^{13}C-NMR (100 MHz, $CDCl_3$) δ: 167.3, 151.0, 131.7, 119.7, 113.9, 51.8.

2,6-Diaminotoluene (Table 2, Entry 11)[64]

^{1}H-NMR (400 MHz, $CDCl_3$) δ: 6.84 (t, J = 8.0 Hz, 1H), 6.20 (d, J = 8.0 Hz, 2H), 3.56 (s, 4H), 1.98 (s, 3H). ^{13}C-NMR (100 MHz, $CDCl_3$) δ: 145.3, 126.9, 107.4, 106.8, 10.3.

Aminonaphthalene (Table 2, Entry 12)[65]

^{1}H-NMR (400 MHz, DMSO-d6) δ: 7.95 (m, 1H), 7.73 (m, 1H), 7.39 (m, 2H), 7.22 (m, 2H), 6.80 (m, 1H). ^{13}C-NMR (100 MHz, DMSO-d6) δ: 143.3, 134.8, 128.0, 126.2, 125.4, 124.2, 121.4, 118.1, 109.5.

4-Aminobiphenyl (Table 2, Entry 13)[58]

^{1}H-NMR (400 MHz, $CDCl_3$) δ: 7.34 (m, 5H), 7.53 (m, 4H). ^{13}C-NMR (100 MHz, $CDCl_3$) δ: 144.79, 129.58, 129.06, 123.17, 120.52, 116.25, 115.47, 115.26.

2,7-Diaminofluorene (Table 2, Entry 14)[66]

^{1}H-NMR (400 MHz, $CDCl_3$) δ: 7.75 (d, 3 $J_{H,H}$ = 7.0 Hz, 4 H), 7.46 (t, 3 $J_{H,H}$ = 7.3 Hz, 2 H), 7.42–7.38 (m, 6 H), 7.28–7.23 (m, 6 H), 7.17–7.13 (m, 4 H), 6.89–6.86 (m, 2 H), 6.66 (dd, 3 $J_{H,H}$ = 8.0, 4 $J_{H,H}$ = 1.9 Hz, 2 H), 3.62 (s, 2 H). ^{13}C-NMR (100 MHz, $CDCl_3$): δ = 167.8, 149.7, 143.7, 139.9, 137.1, 136.4, 130.6, 129.6, 129.3, 128.5, 128.2, 128.0, 119.9, 119.2, 118.0, 36.8.

4-Cyanoaniline (Table 2, Entry 15)[58]

^{1}H-NMR (400 MHz, $CDCl_3$) δ: 7.41 (d, J = 8.36 Hz, 2H), 6.62 (d, J = 11.48 Hz, 2H), 4.13 (br. s, 2H). ^{13}C-NMR (100 MHz, $CDCl_3$) δ: 150.45, 133.96, 120.20, 114.58, 100.50.

5-Amino-2-chlorobenzonitrile (Table 2, Entry 16)[67]

^{1}H-NMR (400 MHz, $CDCl_3$) δ: 7.24 (d, 1H), 6.91 (d, 1H), 6.8 (dd, 1H), 3.91 (s, 2H).

2,6-Dimethylaniline (Table 2, Entry 17)[68]

^{1}H-NMR (400 MHz, $CDCl_3$) δ: 6.83 (2H, d, J = 7.5 Hz), 6.46 (1H, t, J = 7.5 Hz), 4.49 (2H, br s), 2.12 (6H, s). ^{13}C-NMR (100 MHz, $CDCl_3$) δ: 144.16, 127.81, 120.60, 115.89, 17.85.

Cyclohexylamine (Table 2, Entry 18)[69]

^{1}H-NMR (400 MHz, $CDCl_3$) δ: 2.67-2.58 (m, 1H), 2.01-1.56(m, 6H), 1.32-0.98 (m, 4H); ^{13}C-NMR (100 MHz, $CDCl_3$) δ: 49.78, 36.01, 25.00, 24.46.

Aminohexane (Table 2, Entry 19)[61]

^{1}H-NMR (400 MHz, $CDCl_3$) δ: 2.69 (t, *J*=6.5 Hz, 2H), 1.50-1.05 (m, 10H), 0.89 (t, *J*=5.6 Hz, 3H). ^{13}C-NMR (100 MHz, $CDCl_3$) δ: 42.3, 34.1, 31.7, 26.3, 22.8, 14.0.

Nitro-4-(vinyloxy)benzene (Table 5, Entry 1)[70]

^{1}H-NMR (400 MHz, $CDCl_3$) δ 4.72 (dd, J = 6.0,2.0 Hz, 1H), 5.02 (dd, J = 13.6, 2.0 Hz, 1H), 6.70 (dd, J = 13.6, 6.0 Hz, 1H), 7.10 (m, 2H), 8.26 (m, 2H); ^{13}C-NMR(100 MHz, $CDCl_3$): δ 99.1, 116.3, 125.8, 142.9, 145.8, 161.5

1-Nitro-4-(prop-2-ynyloxy)benzene (Table 5, Entry 2)[71]

^{1}H-NMR (400 MHz, $CDCl_3$): 8.22 (d, J = 9.5 Hz, 2H), 7.05 (d, J = 9.5 Hz, 2H), 4.79 (d, J = 2.5 Hz, 2H), 2.58 (t, J = 2.5 Hz, 1H). ^{13}C NMR(100 MHz, $CDCl_3$): 162.3, 142.2, 125.8, 115.0, 77.1, 76.7, 56.3

4-Allyloxyaniline (Table 5, Entry 1)[72]

^{1}H-NMR (400 MHz, $CDCl_3$) δ: 6.62 (d, J=6.2 Hz, 2H), 6.51 (d, J=6.2 Hz, 2H), 5.89 (ddt, J=16.3 Hz, 11.9 Hz, 2.8 Hz, 1H), 5.16 (d, J=16.3 Hz, 1H), 4.97 (d, J=11.9 Hz, 1H), 4.21 (d, J=2.8 Hz, 2H). 13C-NMR (100 MHz, $CDCl_3$) δ: 152.0, 140.3, 134.1, 117.5, 116.7, 116.2, 69.9.

4-(Ethynyloxy)aniline (Table 5, Entry 2)[73]

^{1}H-NMR (400 MHz, $CDCl_3$): δ 7.29 (d, 2H, J = 8.64 Hz), 6.59 (d, 2H, J = 8.67 Hz), 3.81 (s, 2H), 2.96 (s, 1H). ^{13}C-NMR (100 MHz, $CDCl_3$): δ 146.98, 133.41, 114.53, 111.21, 84.36, 74.89.

4-Benzyloxyaniline (Table 5, Entry 3)[72]

^{1}H-NMR (400 MHz, $CDCl_3$) δ: 7.40 (m, 5H), 6.85 (d, *J*=8.7 Hz, 2H), 6.66 (s, *J*=8.7 Hz, 2H), 5.02 (s, 2H), 3.37 (s, 2H). ^{13}C-NMR (100 MHz, $CDCl_3$) δ: 152.0, 140.3, 137.6, 128.4, 127.7, 127.4, 116.3, 116.2, 70.9

Aminoacetophenone (Table 5, Entry 4)[74]

^{1}H-NMR (400 MHz, $CDCl_3$) δ: 7.71 (1H, d, *J* = 8.0 Hz), 7.30–7.10 (3H, m), 6.76 (1H, d, *J* = 8.0 Hz), 6.53 (1H, t, *J* = 8.0 Hz), 2.50 (3H, s). ^{13}C-NMR (100 MHz, $CDCl_3$) δ: 200.15, 151.04, 134.17, 132.22, 116.85, 114.38, 27.84

References

1. Mori, K.; Hara, T.; Mizugaki, T.; Ebitani, K.; Kaneda, K. *J. Am. Chem. Soc.* **2004**, *126*, 10657-10666.

2. Wittmann, S.; Schatz, A.; Grass, R. N.; Stark, W. J.; Reiser, O. A. *Angew. Chem. Int. Ed. Engl.* **2010**, *49*, 1867-1870.

3. Mori, K.; Hara, T.; Mizugaki, T.; Ebitani, K.; Kaneda, K. *J. Am. Chem. Soc.* **2004**, *126*, 10657-10666.

4. Karan, N. S.; Keller, A. M.; Sampat, S.; Roslyak, O.; Arefin, A.; Hanson, C. J.; Casson, J. L.; Desireddy, A.; Ghosh, Y.; Piryatinski, A.; Iyer, R.; Htoon, H.; Malko, A. V.; Hollingsworth, J. A. *Chem Sci* **2015**, *6*, 2224-2236.

5. Wei, G. F.; Liu, Z. P. *Chem Sci* **2015**, *6*, 1485-1490.

6. Priebe, J. B.; Radnik, J.; Lennox, A. J. J.; Pohl, M.-M.; Karnahl, M.; Hollmann, D.; Grabow, K.; Bentrup, U.; Junge, H.; Beller, M.; Brückner. *ACS Catal.* **2015**, *5*, 2137-2148.

7. Stevens, P. D.; Li, G.; Fan, J.; Yen, M.; Gao, Y. *Chem. Commun.* **2005**, *35*, 4435-4437.

8. Bradley, M. J.; Biacchi, A. J.; Schaak, R. E. *Chem. Mater.* **2013**, *25*, 1886-1892.

9. Buck, M. R.; Bondi, J. F.; Schaak, R. E. *Nat. Chem.* **2012,** *4*, 37-44.

10. Sun, X.; Lin, L.; Li, Z.; Zhang, Z.; Feng, J. **2009,** *63*, 2306-2308.

11. Maniecki, T. P.; Mierczynski, P.; Maniukiewicz, W.; Bawolak, K.; Gebauer, D.; Jozwiak, W. K. *Catal. Lett.* **2009**, *130*, 481-488.

12. Choi, S.-W.; Katoch, A.; Sun, G.-J.; Kim, S. S. *Sensors and Actuators B* **2013**, *181*, 446-453.

13. Lu, A. H.; Salabas, E. L.; Schuth, F. *Angew. Chem. Int. Ed. Engl.* **2007**, *46*, 1222-1244.

14. Wang, D.; Astruc, D. *Chem. Rev.* **2014**, *114*, 6949-6985.

15. Polshettiwar, V.; Luque, R.; Fihri, A.; Zhu, H.; Bouhrara, M.; Basset, J. M. *Chem. Rev.* **2011**, *111*, 3036-3075.

16. Gawande, M. B.; Branco, P. S.; Varma, R. S. *Chem. Soc. Rev.* **2013**, *42*, 3371-3393.

17. Lim, C. W.; Lee, I. S. *Nano Today* **2010**, *5*, 412-434.

18. Vernekar, A. A.; Patil, S.; Bhat, C.; Tilve, S. G. *RSC Adv.* **2013,** *3*, 13243.

19. Kim, D.; Guengerich, F. P. *Annu. Rev. Pharmacol. Toxicol.* **2005**, *45*, 27-49.

20. Tafesh, A. M.; Weiguny, J. *Chem. Rev.* **1996**, *96*, 2035-2052.

21. Merlic, C. A.; Motamed, S.; Quinn, B. *J. Org. Chem.* **1995**, *60*, 3365-3369.

22. Wegener, G.; Brandt, M.; Duda, L.; Hofmann, J.; Klesczewski, B.; Koch, D.; Kumpf, R. J.; Orzesek, H.; Pirkl, H. G.; Six, C.; Steinlein, C.; Weisbeck, M. *Appl. Catal. A: Gen.* **2001**, *221*, 303-335.

23. Kantam, M. L.; Chakravarti, R.; Pal, U.; Sreedhar, B.; Bhargava, S. *Adv. Synth. Catal.* **2008**, *350*, 822-827.

24. Mandal, P. K.; McMurray, J. S. *J. Org. Chem.* **2007**, *72*, 6599-6601.

25. Corma, A.; Serna, P.; Concepcion, P.; Calvino, J. J. *J. Am. Chem. Soc.* **2008**, *130*, 8748-8753.

26. Maity, P.; Basu, S.; Bhaduri, S.; Lahiri, G. K. *Adv. Synth. Catal.* **2007**, *349*, 1955-1962.

27. Takasaki, M.; Motoyama, Y.; Higashi, K.; Yoon, S. H.; Mochida, I.. *Org. Lett.* **2008**, *10*, 1601-1604.

28. Corma, A.; Serna, P. *Science* **2006**, *313*, 332-334.

29. He, L.; Wang, L. C.; Sun, H.; Ni, J.; Cao, Y.; He, H. Y.; Fan, K. N. *Angew. Chem. Int. Ed. Engl.* **2009**, *48*, 9538-9541.

30. Yamane, Y.; Liu, X.; Hamasaki, A.; Ishida, T.; Haruta, M.; Yokoyama, T.; Tokunaga, M.. *Org. Lett.* **2009**, *11*, 5162-5165.

31. Jagadeesh, R. V.; Surkus, A. E.; Junge, H.; Pohl, M. M.; Radnik, J.; Rabeah, J.; Huan, H.; Schunemann, V.; Bruckner, A.; Beller, M. *Science* **2013**, *342*, 1073-1076.

32. Wienhofer, G.; Baseda-Kruger, M.; Ziebart, C.; Westerhaus, F. A.; Baumann, W.; Jackstell, R.; Junge, K.; Beller, M. *Chem. Commun.* **2013**, *49*, 9089-9091.

33. Westerhaus, F. A.; Jagadeesh, R. V.; Wienhofer, G.; Pohl, M. M.; Radnik, J.; Surkus, A. E.; Rabeah, J.; Junge, K.; Junge, H.; Nielsen, M.; Bruckner, A.; Beller, M. *Nat. Chem.* **2013**, *5*, 537-543.

34. Shi, Q.; Lu, R.; Lu, L.; Fu, X.; Zhao, D. *Adv. Synth. Catal.* **2007**, *349*, 1877-1881.

35. Blaser, H.-U.; Steiner, H.; Studer, M. *ChemCatChem* **2009**, *1*, 210-221.

36. Mohapatra, S. K.; Sonavane, S. U.; Jayaram, R. V.; Selvam, P. Tetrahedron Lett. **2002**, 43, 8527-8529.

37. Gawande, M. B.; Rathi, A. K.; Branco, P. S.; Nogueira, I. D.; Velhinho, A.; Shrikhande, J. J.; Indulkar, U. U.; Jayaram, R. V.; Ghumman, C. A.; Bundaleski, N.; Teodoro, O. M. *Chem. Eur. J.* **2012**, 18, 12628-12632.

38. Kim, J. H.; Park, J. H.; Chung, Y. K.; Park, K. H. *Adv. Synth. Catal.* **2012**, *354*, 2412-2418.

39. Vasilikogiannaki, E.; Gryparis, C.; Kotzabasaki, V.; Lykakis, I. N.; Stratakis, M. *Adv. Synth. Catal.* **2013**, *355*, 907-911.

40. Couturier, M.; Tucker, J. L.; Andresen, B. M.; Dube, P.; Negri, J. T. *Org. Lett.* **2001**, *3*, 465-467.

41. Göksu, H.; Ho, S. F.; Metin, Ö, Korkmaz, K.; Mendoza Garcia, A.; Gültekin, M. S.; Sun, S. *ACS Catal.* **2014**, *4*, 1777-1782.

42. Jang, Y.; Kim, S.; Jun, S. W.; Kim, B. H.; Hwang, S.; Song, I. K.; Kim, B. M.; Hyeon, T. *Chem. Commun.* **2011**, *47*, 3601-3603.

43. Jang, Y.; Chung, J.; Kim, S.; Jun, S. W.; Kim, B. H.; Lee, D. W.; Kim, B. M.; Hyeon, T. *Phys. Chem. Chem. Phys.* **2011**, *13*, 2512-2516.

44. Chung, J.; Kim, J.; Jang, Y.; Byun, S.; Hyeon, T.; Kim, B. M. *Tetrahedron Lett.* **2013**, *54* (38), 5192-5196.

45. Lee, J.; Chung, J.; Byun, S. M.; Kim, B. M.; Lee, C. Direct Catalytic C–H. *Tetrahedron* **2013**, *69*, 5660-5664.

46. Bae, I. H.; Lee, I.-H.; Byun, S.; Chung, J.; Kim, B. M.; Choi, T.-L. *J. Polym. Sci., Part A: Polym. Chem.* **2014**, *52*, 1525-1528.

47. Byun, S.; Chung, J.; Jang, Y.; Kwon, J.; Hyeon, T.; Kim, B. M. *RSC Adv.* **2013**, *3*, 16296-16299.

48. Byun, S.; Chung, J.; Lim, T.; Kwon, J.; Kim, B. M. *RSC Adv.* **2014**, *4*, 34084-34088.

49. Wang, H.; Qiao, X.; Chen, J.; Wang, X.; Ding, S. *Mater. Chem. Phys.* **2005**, *94*, 449-453.

50. Fernandez-Lopez, C.; Mateo-Mateo, C.; Alvarez-Puebla, R. A.; Perez-Juste, J.; Pastoriza-Santos, I.; Liz-Marzan, L. M. *Langmuir* **2009**, *25*, 13894-13899.

51. Wang, W.; Huang, Q.; Liu, J.; Zou, Z.; Li, Z.; Yang, H. *Electrochem. Commun.* **2008**, *10*, 1396-1399.

52. Yang, W.; Yang, C.; Sun, M.; Yang, F.; Ma, Y.; Zhang, Z.; Yang, X. *Talanta* **2009**, *78*, 557-564.

Peuckert, M.; Bonzel, H. P. *Surf. Sci.* **1984**, *145*, 239-259.

53. Kim, S.; Kim, E.; Kim, B. M. *Chem. Asian J.* **2011**, *6*, 1921-1925.

54. Bhattacharjya, A.; Klumphu, P.; Lipshutz, B. H. *Org. Lett.* **2015**, *17*, 1122-1125.

55. Corma, A.; Garcia, H. *Chem. Soc. Rev.* **2008**, *37*, 2096-2126.

56. Liang, S.; Jasinski, J.; Hammond, G. B.; Xu, B. *Org. Lett.* **2015**, *17*, 162-165.

57. Bartholomew. *Applied Catalysis A: General* **2001**, *212*, 17-60.

58. Kumar, A.; Purkait, K.; Dey, S. K.; Sarkar, A.; Mukherjee, A. *RSC Advances* **2014**, *4*, 35233-35237.

59. Shen, Q.; Hartwig, J. F. *J. Am. Chem. Soc.* **2006**, *128*, 10028-10029.

60. Kamal, A.; Markandeya, N.; Shankaraiah, N.; Reddy, C. R.; Prabhakar, S.; Reddy, C. S.; Eberlin, M. N.; Silva Santos, L. *Chem. Eur. J.* **2009**, *15*, 7215-7224.

61. Orlandi, M.; Tosi, F.; Bonsignore, M.; Benaglia, M. *Org. Lett.* **2015**, *17*, 3941-3943.

62. Lee, D. Y.; Hartwig, J. F. *Org. Lett.* **2005**, *7*, 1169-1172.

63. Tao, C.-Z.; Li, J.; Fu, Y.; Liu, L.; Guo, Q.-X. *Tetrahedron Lett.* **2008**, *49*, 70-75

64. Wu, G. G.; Chen, F. X.; LaFrance, D.; Liu, Z.; Greene, S. G.; Wong, Y. S.; Xie, J. *Org. Lett.* **2011**, *13*, 5220-5223.

65. Göksu, H. *New J. Chem.* **2015**, *39*, 8498-8504.

66. Rotzler, J.; Vonlanthen, D.; Barsella, A.; Boeglin, A.; Fort, A.; Mayor, M. *Eur. J. Org. Chem.* **2010**, *2010*, 1096-1110.

67. Uthuppu, B.; Aamand, J.; Jorgensen, C.; Kiersgaard, S. M.; Kostesha, N.; Jakobsen, M. H*Anal. Chim. Acta* **2012**, *748*, 95-103.

68. Ntaganda, R.; Dhudshia, B.; Macdonald, C. L.; Thadani, A. N. *Chem. Commun.* **2008**, 6200-6202.

69. Damodara, D.; Arundhathi, R.; Ramesh Babu, T. V.; Legan, M. K.; Kumpaty, H. J.; Likhar, P. R. *RSC Adv.* **2014**, *4*, 22567.

70. Blouin, M.; Frenette, R. *J. Org. Chem.* **2001**, *66*, 9043-9045.

71. Lykakis, I. N.; Efe, C.; Gryparis, C.; Stratakis, M. *Eur. J. Org. Chem.* **2011**, *2011*, 2334-2338.

72. Orlandi, M.; Tosi, F.; Bonsignore, M.; Benaglia, M., *Org. Lett.* **2015**, *17*, 3941-3943.

73. Udumula, V.; Tyler, J. H.; Davis, D. A.; Wang, H.; Linford, M. R.; Minson, P. S.; Michaelis, D. J. *ACS Catal.* **2015**, *5*, 3457-3462.

74. Udumula, V.; Tyler, J. H.; Davis, D. A.; Wang, H.; Linford, M. R.; Minson, P. S.; Michaelis, D. J. *ACS Catal.* **2015**, *5*, 3457-3462.

75. Part of this thesis has been published in *ACS Appl. Mater. Interfaces.* **DOI:** 10.1021/acsami.6b05229

국문초록

재활용 가능한 초상자성 팔라듐-백금-산화철 나노촉매입자의 합성 및 효과적인 니트로 환원 반응 적용

외부 자장에 의한 재활용이 가능한 나노 물질은 실질적인 유기화학 합성의 효과적인 비균질성 촉매로 관심도가높아 지며 연구 되어왔다. 본 연구는 산화철 나노 입자에 팔라듐과 백금의 이종 입자를 고정화 시키며, 그 나노 촉매를 니트로 화합물들에 매우 효과적으로 적용 하는 것이다. 팔라듐-백금-산화철 입자는 구매가 가능한 산화철 입자를 팔라듐, 백금 반응물들과 여러 추가적인 물질에 의하여 쉽게 만들 수 있다. 이러한 팔라듐-백금-산화철 입자는 다양한 니트로 작용기가 있는 화합물을 포함하여 화학선택적 반응에서도 5분만에 높은 수득률을 보여주었다. 더욱이 250번의 재활용 반응에서도 촉매의 활성이 저하되지 않고 반응성이 좋음을 확인하였다.